A Monolithic Programmable Optical Filter for RF-Signal Processing

Erik J. Norberg, Robert S. Guzzon, John S. Parker, Leif A. Johansson and Larry A. Coldren

ECE Department, University of California, Santa Barbara, CA 93106, USA

norberg@ece.ucsb.edu

Abstract—**A monolithic programmable optical filter suitable for dynamic pre-filtering of wide bandwidth RF signal-bands is presented. Bandpass filters have a passband tunable in bandwidth (3-14GHz) and center frequency (0-40GHz). Cascaded filter sections have stopband rejection exceeding 35dB.**

I. INTRODUCTION

All-optical signal processing has the capabilities to reduce latency, power consumption, cost and size, and overcome the inherent bandwidth limitations of its electronic counterparts [1,2]. By rapidly pre-filtering wide bandwidth analog signals in the optical domain the demand on analog-to-digital converstion (ADC) and subsequent digital signal processing (DSP) can be significantly relieved. Such a filter should ideally be highly versatile and synthesize both notch- and bandpass type filters so RF signal bands or signatures quickly can be rejected or isolated for more detailed investigation. It is also desirable that the filter passband be tunable in both bandwidth and center frequency to accommodate varying signal widths and locations in the RF domain, as well as enable tracking and sweeping abilities in the frequency domain, properties that are crucial for electronic warfare (EW) systems. A lattice type filter structure utilizing both Mach-Zehnder interferometers and ring resonators together with optical phase and amplitude control can provide these desired filter characteristics [3]. We have previously demonstrated the basic building block or unit cell of such a lattice filter, integrated in the InGaAsP material system [4]. Similar unit cells have in parallel been suggested and demonstrated on other integration platforms: gain-less silicon-on-insulator (SOI) [5,6] and SOI-IIIV hybrid [7]. More recently, we verified the ability to monolithically cascade these lattice cells to create higher order filters [8]. In this paper, we demonstrate novel functionality of such cascaded lattice filters including flat-topped bandpass filters with passbands tunable in both bandwidth and center frequency.
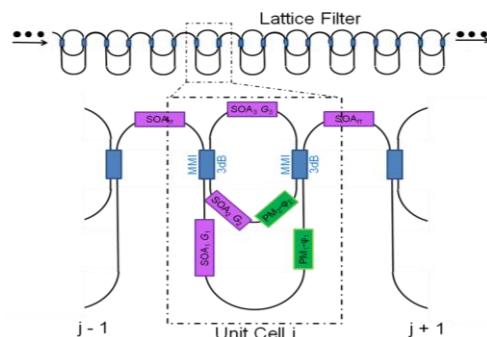
Figure 1. Schematic of the programmable lattice filter and the single unit cell; functional components, SOAs, Phase modulators and couplers have been highlighted.

II. FILTER DESIGN

A. Single Unit Cell

The fundamental filter structure is depicted in Figure 1. *N* cascaded identical filter stages or unit cells make up a one dimensional lattice structure. Every unit cell is designed to be able to synthesize either a pole or a zero. This is achieved by an asymmetrical Mach-Zendher interferometer (MZI) with a feedback path connecting the output to the input, thus creating two different resonator paths, Figure 1. Hence, the complete unit cell response consists of two poles and one zero. However, in favor of stability and control, only one pole or one zero per unit cell is utilized at any one time. The individual pole or zero is isolated by utilizing active gain/absorption elements to shut off different waveguide paths. If the top path of the unit cell is turned off, a single zero results through the remaining MZI path. Alternatively, if one of the MZI paths is shut off, one of the two poles is isolated. By designing the lengths of the different waveguide paths, desired free-spectral-range (FSR) and filter bandwidths are achieved. In this work, the two resonators have a length of 1,750 or 3,500 mm, corresponding to time delays of 21 and 42 ps, or FSRs of 48 and 24 GHz respectively. The MZI was designed with a path difference of 21 ps or FSR of 48 GHz. The pole and zero magnitudes are controlled by balancing the MZI arms or providing resonator gain respectively, while the phase (frequency) is controlled by the phase modulators located in both paths of the MZI.

B. Lattice Filter Operation

The single unit cells are cascaded in an uncoupled fashion with a single waveguide connecting the cells; there is no feedback between the unit cells and the individual unit cell transfer functions are multiplied in a linear fashion. This naturally aids in stability and control of these lattice filter structures as well as simplifying the filter synthesis since the unit cells can be controlled individually. Higher order filters are constructed by programming the unit cells with desired pole or zero magnitudes and phases. Bandpass filters are constructed by utilizing two or more poles; the passband bandwidth can be varied by changing the pole magnitude and adjusting the pole location to maintain a flat passband. Since the unit cell design incorporates two poles with different FSRs, bandpass filters with inherently wider or narrower FSR and bandwidths can be utilized for different bandwidth applications. Zeros can be added to construct elliptical bandpass designs with enhanced filter extinction and roll-off. By using only zeros, notch filters are synthesized. In the current design the FSR of the zero is twice that of the longer ring, thus the zero can also be used to enhance the FSR of the narrower bandwidth bandpass filter by canceling out the neighboring filter order on either side.

In the current design, the device does not include any on-chip modulator, laser source, or detectors. However, using the InGaAsP integration platform, these components could all be integrated together with the filter if an electrical RF-in and or out was desired. However, for many applications, the RF might already be on an optical carrier, where the filter would work as a subsystem in the RF link, e.g. in remote antenna fiber links.

C. Integration Platform

For monolithic integration of the filter structure we utilize the InP-InGaAsP material system. This has the advantage of on-chip gain through semiconductor amplifiers (SOAs) and effective and quick phase control using current injected phase modulators. Of course, utilizing on-chip gain, the impact on the spur-free dynamic range (SFDR) through saturation effects in the SOA must be considered. It can be shown that the ratio of intermodulation distortion to signal power is proportional to the inverse of the squared SOA saturation power [9]. Thus the SFDR is proportional to the squared saturation power, which in turn is proportional to the quantum well confinement factor. For this reason, we utilize an offset quantum well (OQW) integration platform which has a lower confinement factor compared to centered multi quantum well (MQW) structures. We measured the optical 3dB-saturation power of our SOAs to be 11.4 dBm; this should be compared to 15 dBm which has been calculated to have an SFDR number in the range 105-115 dB/Hz$^{2/3}$ (lower end for low frequencies) for a commercial InGaAsP QW SOA [10]. We do have the ability to push the saturation power higher by further reducing the confinement factor, 20 dBm having previously been demonstrated [11]. This suggests SFDR numbers as high as 115-125 dB/Hz$^{2/3}$, which is sufficient for most radar applications. The re-programming and tuning time of the filter is ultimately limited by the response time of the gain and phase controllers, which here are governed by the carrier lifetime suggesting extremely fast tuning speeds in the nano-second range [12]. This is crucial for fast tracking and sweeping in the RF domain which is important to many applications.

In order to avoid radiation loss from waveguide bends and keep the fabrication complexity to a minimum, deeply etched waveguides was used for the entire device. For coupling, 3dB restrictive multi-mode-interference (MMI) couplers with a measured total insertion loss of ~1.0 dB/coupler were used everywhere. More details on the fabrication and integration platform have been reported elsewhere [13]. Figure 2 shows a fabricated lattice filter with four cascaded unit cells that have been wire-bonded to a carrier; the device size measures 1.5 x 3.5 mm.

Figure 2.   Scanning electron microscope image of a fabricated device containing four unit cells; device has been wirebonded to a carrier.

III.   EXPERIMENT AND DISCUSSION

A. Experiment

In this work we investigated a lattice filter structure consisting of a four cascaded unit cells, Figure 2. In order to demonstrate the filtering function of our device, we input a band limited noise spectrum into the device and measure the output in high resolution (10 MHz), utilizing a heterodyne detection scheme. The band limited noise spectrum simulates a wide bandwidth single sideband RF-signal band that has been carrier suppressed. A schematic of the measurement is shown in Figure 3. The noise spectrum is generated by an amplified spontaneous emission (ASE) source and is amplified by erbium doped fiber amplifiers (EDFAs) and sent through a circulator connected to a fiber grating (FBG) that has a 44 GHz wide reflection bandwidth. The filtered signal is down converted using a tunable laser placed just to the side of the initial noise spectrum at 1553.152nm, inset Figure 3. A 40 GHz photodiode (PD), with a 38 GHz broadband amplifier and a 50 GHz electrum spectrum analyzer (ESA) is used to image the device output in the electrical domain. All data was normalized to the throughput (w/o device) in order to eliminate ripples in the FBG spectrum. The added receiver noise was subtracted from the measured data. An optical spectrum analyzer (OSA) was used in parallel to monitor the optical domain; however, the OSA does not have the resolution necessary to truthfully resolve the filter shapes. All measurements were done continuous wave (CW) in room-temperature.
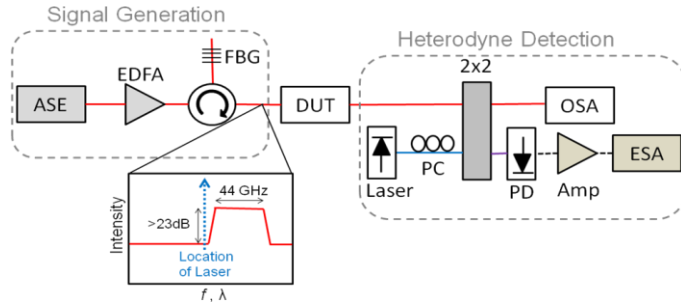
Figure 3. Schematic of experimental setup. Inset spectrum shows the generated signal and where the local oscillator laser is located in the heterodyne detection.
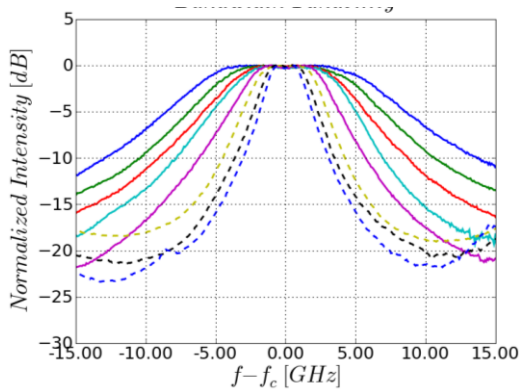

Figure 4. 2nd order bandpass filter with variable passband bandwidth. Solid and dashed lines indiate the use of the shorter or longer resonator respectivly.

B. Results and Discussion

Utilizing two out of four unit cells, a variable bandwidth 2nd order bandpass filter is demonstrated in Figure 4. For easy comparison, the filters have been normalized in frequency from the 20-25 GHz range down to zero. The bandwidth is varied by changing the pole magnitudes from 0.55 to 0.75 (found by fitting data to simulations) while adjusting the phase difference between the poles to maintain the flat passband. The ripple is kept less then 0.5dB for all filters. The tuning is completely continuous but illustrated with a few discrete steps for clarity. Since the pole magnitudes are varied, the filter extinction and roll-off also change accordingly. Thus, it becomes necessary to keep a lower bound on the pole magnitude to maintain sufficient filtering efficiency. The shorter resonator configuration with a FSR of 48 GHz is here utilized for filtering in the 5-14 GHz bandwidth regime (solid lines in figure 4), while the longer resonators with FSR of 24 GHz are utilized for 3-5 GHz (dashed lines in Figure 4). For many RF-applications, filter bandwidths even narrower than the 3 GHz demonstrated here are desired. This requires longer resonator and MZI delays. However, the principle of the demonstrated filter operation does not change. In this current design we have considerable excess gain, so by keeping the same SOA gain but moving to a lower loss InGaAsP integration platform (basically reducing p-cladding overlap), e.g. [14], 10 cm resonator delays with 100 MHz filter bandwidths are feasible. The shorter resonator delays will however still be crucial to achieve a broad operation range

(governed by the filter FSR) by removing the narrowly spaced neighboring filter orders of the longer delays.

The second important functionality beside a variable filter bandwidth is the ability to tune the center frequency of the passband. This is demonstrated in Figure 5 using a 2nd order bandpass filter tuned from 9 to 37 GHz. The tuning can extend further but above 40 GHz the receiver noise becomes too large. In fact, all the poles and zeros have more then 2π of phase tuning, effectively meaning that the filter can work anywhere in the gain bandwidth (5 THz wide). Thus, the filter operation range is limited by the FSR, here 48 GHz. The small peaks showing in the stopband are not part of the filter but rather an artifact of the measurement. These peaks are caused by the laser beating with the neighboring filter order to the left of the laser since the FBG extinction ratio is limited; see inset Figure 3. Note that the added center frequencies of the filter passband and the peak in the stopband always equal the filter FSR, as would be expected for this phenomena.

For improved extinction and roll-off, higher order filters can be utilized. Figure 6 shows the improvement in using four instead of two unit cells. With four poles, a 2nd order bandpass filter was cascaded twice, enhancing filter roll off and stopband rejection to almost 40 dB. Again, the limitation of the measurement setup is evident; at high extinctions many low intensity peaks generated by the measurement are revealed in the stopband, e.g. the peak at -12 GHz (at 10 GHz before frequency normalization) is caused by an internal interference in the tunable laser.
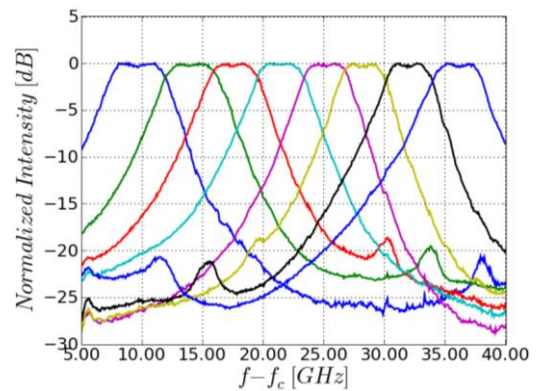

Figure 5. Frequency tunability of a 2nd order bandpass filter.
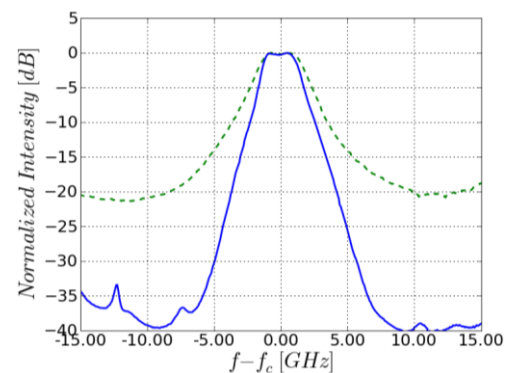

Figure 6. Comparison of bandpass filters constructed from 2 poles (dashed) and 4 poles (solid).

For the four unit cell long lattice filter investigated here, the end-to-end loss (not including fiber coupling losses) in the passband is generally zero or has slight gain. This suggests that the number of lattice cells could be increased further. For example, going of Figure 6, a lattice with only 8 unit cells would produce a stopband rejection of ~75 dB. The only limitation of longer lattices seems to lie in practical interfacing and control, since additional bias parameters are introduced with added unit cells. Thus it would be desirable to interface the lattice filter with a field-programmable gate array (FPGA) controller to ease the filter synthesis in the future.

IV. CONCLUSION

We have presented a programmable optical filter constructed as a lattice of identical unit cells. The uncoupled unit cells give rise to independently programmable zeros and poles which can freely be placed in the complex plane. We have demonstrated a 2nd order bandpass filter tunable in both bandwidth and center frequency, and shown that longer lattices can be used to enhance the filter roll-off and stopband rejection. This kind of filter would be suitable for signal processing of wide bandwidths RF signal-bands in the optical domain.

REFERENCES

[1] J. Yao, "Microwave Photonics," *J. of Lightw. Technol.*, vol. 27, no. 3, Feb. 2009.

[2] J. Campany, B. Ortega, D. Pastor, "A tutorial on Microwave Photonic Filters," *J. of Lightw. Technol.*, vol. 24, no. 1, Jan 2006.

[3] C. K. Madsen., J. H. Zhao, Optical Filter Design and Analysis : A Signal Processing Approach, Whiley-Interscience, Chap.6.

[4] E. J. Norberg, R. S. Guzzon, S. C. Nicholes, J. S. Parker and L. A. Coldren, "Programmable Photonic Lattice Filters in InGaAsP-InP," *Photonics Technology Letters*, vol. 22, no.2, pp. 109-111, Jan. 2010.

[5] P. Toliver *et al.*, "A programmable Optical Filter Unit Cell Element for High Resolution RF Signal Processing in Silicon Photonics," Proc. *OFC/NFOEC,* OWJ4, 2010.

[6] S. Ibrahim *et al.,* " Fully Reconfigurable Silicon Photonic Lattice Filters with Four Cascaded Unit Cells", Proc. *OFC/NFOEC,* OWJ4, 2010.

[7] HW Chen, A. W. Fang, J. Bovington, J. Peters and J. Bowers, "Hybrid silicon tunable filter based on a Mach-Zehnder interferometer and ring resonantor," *Proc. Microwave Photonics*, pp. 1-4, 2009.

[8] E. J. Norberg, R. S. Guzzon, J. S. Parker and L. A. Coldren, "Programmable Photonic Filters from Monolithic Cascaded Filter Stages," *IPR,* 2010, unpublished.

[9] Y. C. Chung, J. M. Wiesenfeld, G. Raybon, U. Koren, "Intermodulation Distortion in a Multiple-Quamum-Well Semiconductor Optical Amplifier," *Photon. Technol. Lett.,* vol. 3, no. 2, Feb. 1991.

[10] P. Berger, J. Bourderionnet, M. Alouini, F. Bretenaker, and D. Dolfi, "Theoretical Study of Spurious-Free Dynamic Range on a Tunable Delay Line based on Slow Light in SOA," *Opt. Exp.*, vol. 17, no. 22, 2009.

[11] J. Raring, E. Skogen, M. Mašanovic, S. DenBaars, and L. Coldren, "Demonstration of high saturation power/high gain SOAs using quantum well intermixing and MOCVD regrowth," *IEE Electronics Letts.* vol.41, pp. 1345-1346, Nov. 2005.

[12] L. A. Coldren and S. W. Corzine, Diode Lasers and Photonics Integrated Circuits, Whiley-Interscience, 1995, pp 218.

[13] E. J. Norberg, R. S. Guzzon, S. C. Nicholes, J. S. Parker and L. A. Coldren, "Programmable photonic filters fabricated with deeply etched waveguides," *Proc. Indium Phosphide & Related Materials*, pp.163-166, 2009.

[14] T. Uitterdijka, H van Bruga, F. H. Groena, H. J. Frankenaa, "Integrable Polarization Insensitive InGaAsP/InP Mach-Zehnder switch,"*Proc. IPR*, pp.486-489, 1996.